第 31 卷第 5 期
2015 年 5 月

无 机 化 学 学 报
CHINESE JOURNAL OF INORGANIC CHEMISTRY

Vol.31 No.5
857-864

咪唑–芳香多羧酸金属有机骨架化合物的合成、结构及性质

钱岩涛　彭烨栋　章文伟*

(配位化学国家重点实验室,南京大学化学化工学院,南京　210093)

摘要：以 5-(1*H*-咪唑)异酞酸(H_2L)为配体,在水热条件下合成了 3 个金属有机框架化合物:$[PrL(HL)(H_2O)_2]\cdot H_2O$ (**1**),$Er(H_{0.5}L)_2$ (**2**)和$[CoL(H_2O)_2]\cdot H_2O$ (**3**)。单晶 X-射线衍射测试结果表明,3 个化合物都属于单斜晶系,$P2_1/c$ 空间群。化合物 **1** 中,Pr^{3+}为九配位,而化合物 **2** 和 **3** 中,Er^{3+}和 Co^{2+}均为六配位。在镧系配合物 **1** 和 **2** 中,配体中氮原子未参与配位。**1** 为 2D 折叠形结构,**2** 为 3D 框架结构。在过渡金属配合物 **3** 中,氮原子与 Co^{2+}配位,这有助于形成平面二维结构。化合物 **1** 和 **3** 通过分子间 π-π 堆积,进一步形成 3D 结构。3 个化合物均展现出较好的热稳定性。

关键词：金属有机骨架化合物；过渡金属；镧系元素；水热合成；晶体结构

中图分类号：O614.33+4；O614.344；O614.81+2　　**文献标识码**：A　　**文章编号**：1001-4861(2015)05-0857-08

DOI:10.11862/CJIC.2015.148

Syntheses, Structures and Properties of Metal-Organic Frameworks Based on Imidazolyl-Aromatic Multi-Carboxylate Acid Ligands

QIAN Yan-Tao　PENG Ye-Dong　ZHANG Wen-Wei*

(*State Key Laboratory of Coordination Chemistry, School of Chemistry and Chemical Engineering, Nanjing University, Nanjing* 210093, *China*)

Abstract: Three metal-organic frameworks, namely $[PrL(HL)(H_2O)_2]\cdot H_2O$ (**1**), $Er(H_{0.5}L)_2$ (**2**), and $[CoL(H_2O)_2]\cdot H_2O$ (**3**) (H_2L =5-(1*H*-imidazol-1-yl)isophthalic acid), have been synthesized under hydrothermal condition. Single crystal X-ray diffraction indicates that all the three complexes belong to the monoclinic space group $P2_1/c$. The Pr^{3+} ions in **1** are nine-coordinated, while the Er^{3+} ions in **2** and Co^{2+} ions in **3** are both six-coordinated. In the lanthanide complex **1** and **2**, the nitrogen atom does not coordinate with any metal ions. Complex **1** shows a 2D folding framework, while complex **2** exhibits a 3D network. In the transition metal complex **3**, the nitrogen atom coordinates with Co^{2+}, which helps to form a flat 2D framework. Complex **1** and **3** are further packed into 3D framework by the intermolecular π-π interactions. All the three complexes display good thermal stability. CCDC: 1005562, **1**; 1005563, **2**; 1005564, **3**.

Key words: metal-organic framework; transition metal; lanthanide; hydrothermal synthesis; crystal structure

0 Introduction

In recent years, metal organic frameworks (MOFs) have been widely synthesized not only for gorgeous structures, but also for lots of their potential uses, such as gas storage, ion exchange, separation, catalysis and so on[1]. However, it is still a challenge to predict and control the final architectures of the desired crystalline products due to the structural uncertainty and diversity, since the network formation is sensitive

收稿日期:2015-01-27。收修改稿日期:2015-03-27。

国家自然科学基金(No.51173075)资助项目。

*通讯联系人。E-mail:wwzhang@nju.edu.cn

to many factors such as organic ligands, metal ions, metal-to-ligand ratio, template, solvents, pH value, reaction temperature, and the method of crystallization, etc[2-6].

Among them, organic ligands and metal ions are the two major aspects that should be considered in the construction of MOFs. As it is known, multicarboxylate ligands, such as 1,4-benzenedicarboxylate, 1,3,5-benzenetribenzoate, 3,3′,5,5′-biphenyl tetracarboxylate, 1,1′-ethynebenzene-3,3′,5,5′-tetracarboxylate, 1,1′-butadiynebenzene-3,3′,5,5′-tetracarboxylate, have been widely used to build MOFs with multi-dimensional architectures and interesting properties because of their rich and reliable coordination modes[7-8]. Moreover, ligands with nitrogen donors, such as 3,5-diethyl-1,2,4-triazole, 1,4-bis(1-imidazolyl)benzene, 1,4-di(1*H*-imidazol-4-yl)benzene, have also shown great ability in the assembly of MOFs with novel structures and natures[9]. Taking account the facts above, we designed and synthesized a planar-shaped ligand containing both O and N donors, named 5-(1*H*-imidazol-1-yl) isophthalic acid (H_2L) (Scheme 1), and further synthesized with different lanthanide and transition metal ions to give complexes $[PrL(HL)(H_2O)_2]\cdot H_2O$ (**1**), $Er(H_{0.5}L)_2$ (**2**) and $[CoL(H_2O)_2]\cdot H_2O$ (**3**) with diverse structures. Herein we present the solvothermal synthesis, crystal structures, and luminescent properties of these three novel coordination polymers.

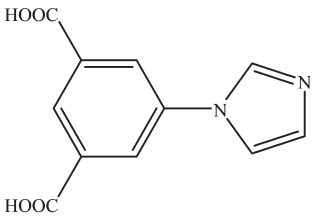

Scheme 1 Molecular structure of ligand H_2L

1 Experimental

1.1 Materials and measurements

All commercially available chemicals were of analytical grade and used as received without further purification. Elemental analyses (C, H and N) were carried out on a Perkin-Elmer 240 analyzer. The FTIR spectra were obtained on a VECTORTM 22 spectrometer with KBr pellet in the 400~4 000 cm^{-1} region. ^1H NMR spectra were recorded on a Bruker DRX-500 spectrometer at room temperature with tetramethylsilane as an internal reference. TGA-DTA diagrams were recorded by a CA Instruments DTA-TGA 2960 type simultaneous analyzer heating from 293 to 973 K in nitrogen atmosphere at a rate of 20 $K\cdot min^{-1}$. Powder X-ray diffraction (PXRD) data were recorded on a Shimadzu XRD-6000 X-ray diffractometer with Cu $K\alpha$ (λ=0.154 18 nm) radiation at room temperature with a scan speed of $5°\cdot min^{-1}$ and a step size of 0.02° in 2θ.

1.2 Synthesis

1.2.1 Synthesis of the ligand H_2L

The synthesis of H_2L was performed according to the literature[10]. A mixture of K_2CO_3 (6.00 g 0.043 mol), 5-iodoisophthalic acid (4.30 g. 0.015 mol), imidazole (5.20 g, 0.076 mol) and $CuSO_4\cdot 5H_2O$ (0.010 g, 40 μmol) were blended sufficiently. The powdered reactant mixture was transferred into 20 mL Teflon-lined autoclave, which was sealed and heated at 200 ℃ for 10 h. After cooling down, the reaction mixture was dissolved in water and filtered off. The pH value of filtrate was adjusted with dilute hydrochloric acid to 2.0~3.0. The white precipitate was filtered and washed by water then by ethanol. The production was evaporated to dryness in vacuum. (Yield: 65%, based on 5-iodoisophthalic acid). ^1H NMR [$(CD_3)_2SO$] δ: 8.45 (s, 1H), 8.40 (s, 1H), 8.32 (s, 2H), 7.93 (s, 1H), 7.15 (s, 1H); IR (KBr pellet, cm^{-1}): 3 430 (w), 3 112 (s), 2 502 (w), 1 944 (w), 1 701 (s), 1 592 (m), 1 391 (m), 1 233 (s), 1 064 (m), 855 (m), 761 (m), 693 (m). MS: *m/z* 231.42 (Calcd. 231.13).

1.2.2 Synthesis of complex $[PrL(HL)(H_2O)_2]\cdot H_2O$ (**1**)

A mixture of $Pr(NO_3)_3\cdot 6H_2O$ (29.1 mg, 0.1 mmol), H_2L (4 mg, 0.017 2 mmol) and H_2O (6 mL) was under ultrasound for 5 minutes and then put in a 10 mL Teflon-lined stainless steel container, which was sealed and heated at 160 ℃ for 72 h. After cooling to room temperature, light brown crystals were collected (Yield: 17.7% based on H_2L). Anal. Calcd. for $C_{22}H_{19}N_4O_{11}Pr$ (%): C, 40.22; H, 2.89; N, 8.54. Found (%): C, 40.23; H, 2.90; N, 8.52. IR (KBr pellet, cm^{-1}):

3 404 (w), 3 150 (w), 3 118 (m), 1 625 (m), 1 552 (s), 1 457 (m), 1 387 (s), 1 249 (s), 1 058 (m), 875 (m), 783 (m), 666 (m).

1.2.3 Synthesis of complex $Er(H_{0.5}L)_2$ (**2**)

A mixture of $Er(NO_3)_3\cdot 6H_2O$ (29.1 mg, 0.1 mmol), H_2L (18 mg, 0.077 6 mmol) and H_2O (6 mL) was under ultrasound for 5 min and then put in a 10 mL Teflon-lined stainless steel container, which was sealed and heated at 200 ℃ for 12 h. After cooling to room temperature, brown crystals were collected (Yield: 41.0% based on H_2L). Anal. Calcd. for $C_{22}H_{13}N_4O_8Er$ (%): C, 42.01; H, 2.07; N, 8.90. Found (%): C, 42.22; H, 2.09; N, 8.87. IR (KBr pellet, cm^{-1}): 3 432 (w), 3 164 (m), 3 107 (m), 1 625 (s), 1 548 (s), 1 452 (m), 1 424 (s), 1 367 (m), 1 267 (m), 1 070 (m), 901 (m), 876 (m), 778 (m), 632 (m).

1.2.4 Synthesis of complex $[CoL(H_2O)_2]\cdot H_2O$ (**3**)

A mixture of $Co(NO_3)_2\cdot 6H_2O$ (29.1 mg, 0.1 mmol), H_2L (7 mg, 0.030 2 mmol) and H_2O (6 mL) was under ultrasound for 5 minutes and then put in a 10 mL Teflon-lined stainless steel container, which was sealed and heated at 200 ℃ for 12 h. After cooling to room temperature, red block crystals were collected (Yield: 42.4% based on H_2L). Anal. Calcd. for $C_{11}H_{12}N_2O_7Co$ (%): C, 38.47; H, 3.50; N, 8.16. Found (%): C, 38.45; H, 3.49; N, 8.15. IR (KBr pellet, cm^{-1}): 3 460 (w), 3 146 (s), 3 101 (w), 1 631 (s), 1 581 (s), 1 429 (m), 1 384 (s), 1 261 (m), 1 165 (m), 1 075 (m), 940 (m), 835 (m), 728 (m), 648 (m).

1.3 Single crystal X-ray crystallography

Single crystal X-ray diffraction data were collected on a Bruker Smart Apex Ⅱ CCD diffractiometer using graphite monochromated Mo $K\alpha$ radiation (λ=0.071 073 nm). Data reductions and absorption corrections were performed with the SAINT and SADABS software packages[11], respectively. Structures were solved by a direct method using the SHELXL-97 software package[12]. The non-hydrogen atoms were anisotropically refined using the full-matrix least-squares method on F^2. All hydrogen atoms were put at the calculated positions

Table 1 Crystal data and structure refinements for complexes 1, 2 and 3

Complex	1	2	3
Empirical formula	$C_{21}H_{19}N_4O_{11}Pr$	$C_{22}H_{13}N_4O_8Er$	$C_{11}H_{12}N_2O_7Co$
Formula weight	644.31	628.62	343.16
Crystal system	Monoclinic	Monoclinic	Monoclinic
Space group	$P2_1/c$	$P2_1/c$	$P2_1/c$
a / nm	1.480 4(2)	0.478 78(5)	1.054 0(9)
b / nm	0.796 58(12)	1.443 19(15)	1.658 6(14)
c / nm	2.002 4(3)	1.412 65(15)	0.724 6(6)
β / (°)	101.441(2)	90.824 0(10)	96.102(15)
T / K	296(2)	296(2)	291(2)
V / nm^3	2.314 4(6)	0.976 00(18)	1.259 5(18)
Z	4	2	4
D_c / ($g\cdot cm^{-3}$)	1.849	2.136	1.810
μ / mm^{-1}	2.177	4.365	1.401
F(000)	1 280	676	700.0
θ range for data collection / (°)	1.40~27.49	2.82~27.41	2.45~30.06
Reflns collected	19 762	6 898	11 680
Unique reflns	5 220	2 191	3 026
R_{int}	0.077 7	0.057 0	0.099 1
GOF	1.094	1.092	1.032
R_1[a] / wR_2[b] ($I>2\sigma(I)$)	0.082 8 / 0.229 7	0.086 7 / 0.236 7	0.040 3 / 0.076 4
R_1[a] / wR_2[b] (all data)	0.102 5 / 0.255 0	0.092 7 / 0.250 9	0.054 0 / 0.078 3

[a]$R_1=\sum||F_o|-|F_c||/\sum|F_o|$; [b]$wR_2=\{\sum[w(F_o^2-F_c^2)^2]/\sum[w(F_o^2)^2]\}^{1/2}$

and refined riding on the parent atoms. Crystal data and structure refinement information for the three complexes are listed in Table 1. The main bond lengths and angles are summarized in Table S1.

CCDC: 1005562, **1**; 1005563, **2**; 1005564, **3**.

2 Results and discussion

2.1 Crystal structures

The purities of **1**~**3** are confirmed by powder X-ray diffraction (PXRD) measurements. The PXRD patterns of the as-synthesized products are in good agreement with the simulated ones, indicating that they are in high phase purity (Fig.S1). Single crystal X-ray diffraction indicates that complex **1** belongs to the monoclinic space group $P2_1/c$, with its asymmetric unit consisting of one Pr^{3+} ion, two deprotonated ligands (the carboxylate L^{2-} and the N4-protonated carboxylate HL^-, vide infra), two coordinated H_2O and one guest H_2O. As show in Fig.1a, the Pr^{3+} ion is nine-coordinated to form a distorted tricapped trigonal prism coordination geometry (Fig.4a), in which seven oxygen atoms (O1, O2, O4, O5, O6, O7 and O11) come from the ligands, two oxygen atoms (O9 and O10) from two H_2O molecules. Among the seven oxygen atoms from the two ligands, six are from three bidentately chelated coordinating carboxyl groups, and one from a monodentately carboxyl group (Fig.4a). The Pr-O bond lengths vary from 0.247 4(7) to 0.261 1(7) nm, which are within the range of previously published lanthanide complexes with carboxylic acids as bridging ligands[13]. It should be noted that the two ligands in the asymmetric unit are different, one should be deprotonated as the carboxylate ligand L^{2-} and the other as HL^- since Pr^{3+} ion has positive charge of three. That is to say, the deprotonated ligand HL^- has one more hydrogen atom. Considering the bond lengths of C18-N5 and C24-N5 are different as 0.129 51(119) and 0.138 89(148) nm, respectively, while those of C15-N4 and C3-N4 are almost the same, which are 0.133 45(145) and 0.134 42(146) nm, respectively, the additive H in HL^- should be added on N4 of the imidazole group. Moreover, from Fig.1b, it can be seen that every Pr^{3+} ion connects four ligands and every ligand links two Pr^{3+} ions, generating a 2D folded sheet framework. There are O–H···O hydrogen bonds within the frameworks (O9–H8W···O6), which are detailed in the supporting materials (Fig.S2 and Table S2). Besides the hydrogen bond interactions, π-π interactions also exit between different layers with distances of 0.372 8 and 0.398 0 nm, respectively (Fig.S3),

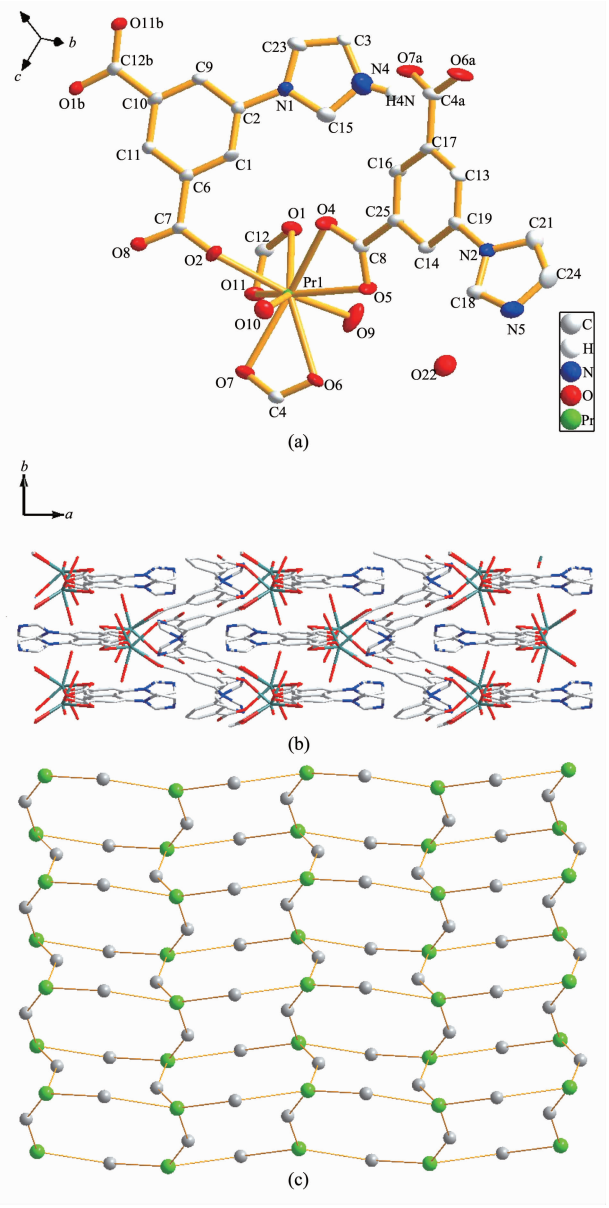

Fig.1 (a) Asymmetric unit of **1** with thermal ellipsoids at 50% probability level (Symmetry codes: a: x, 1.5−y, −0.5+z; b: 2−x, −0.5+y, 1.5+z); (b) Packing structure of **1** along the c axis; (c) Topology of complex **1** (green represents the 4-connected node of Pr^{3+} ion and gray represents the 2-connected node of organic ligand)

leading the 2D folded sheet to a 3D framework. From the view point of topology, **1** can be described as a (4,2)-connected network with Schlfli symbol of ($4^4.6^2$) since each Pr^{3+} ion can be served as a 4-connected node and every ligand can be considered as a 2-connected node, which is shown in Fig.1c.

Complex **2** also belongs to the monoclinic space group $P2_1/c$, and its asymmetric unit consists of half Er^{3+} and one N-protonated carboxylate ligand ($H_{0.5}L^{1.5-}$). It should be noted that the occupancy probability of H3 added to N3 is set 0.5 for charge balance, thus the N-protonated carboxylate ligand in **2** is termed as $H_{0.5}L^{1.5-}$. In complex **2**, six oxygen atoms (O1, O2, O4, O1A, O2A and O4A) from the ligand coordinate to Er^{3+} (Fig.2a), displaying a distorted octahedron (Fig. 4b). Unlike those in complex **1**, the ligand in **2** uses its three oxygen atoms of the two carboxyl groups to coordinate with three Er^{3+} ions in the monodentately and bidentately bridging modes (Fig.4b), and each Er^{3+} ion connects six ligands, leading to a 3D structure with little void space because the imidazole part of the ligand does not participate in the coordination and it fills the channel formed along the *a* axis, which can be seen clearly from its packing structure presented in Fig.2b. As described above, Er^{3+} ion can be served as a 6-connected node and the ligand can be considered as a 3-connected node. Therefore, **2** can be topologically interpreted as a (6,3)-connected net based on the assembly of two different kinds of nodes. Its Schlfli symbol is $(4.6^2)_2(4^2.6^{10}.8^3)$ (Fig.2c).

Complex **3** belongs to the monoclinic space group $P2_1/c$. Its asymmetric unit consists of one Co^{2+} ion, one deprotonated ligand (L^{2-}), two coordinated water and an uncoordinated water. As illustrated in Fig.3a, Co^{2+} in **3** has a distorted octahedral coordination geometry: three oxygen atoms (O1, O2, O3) and one nitrogen atom (N2) from ligand, the other two oxygen atoms (O1W, O2W) from two coordinated water (Fig.4c). Among them, the three coordinated oxygen atoms from two carboxyl groups of the ligand adopt monodentately and bidentately chelated coordinating mode, respectively (Fig.4c). The distance of Co-N bond is 0.204 8(2) nm, and that of Co-O ranges from 0.203 2(2) to 0.230 6(2)

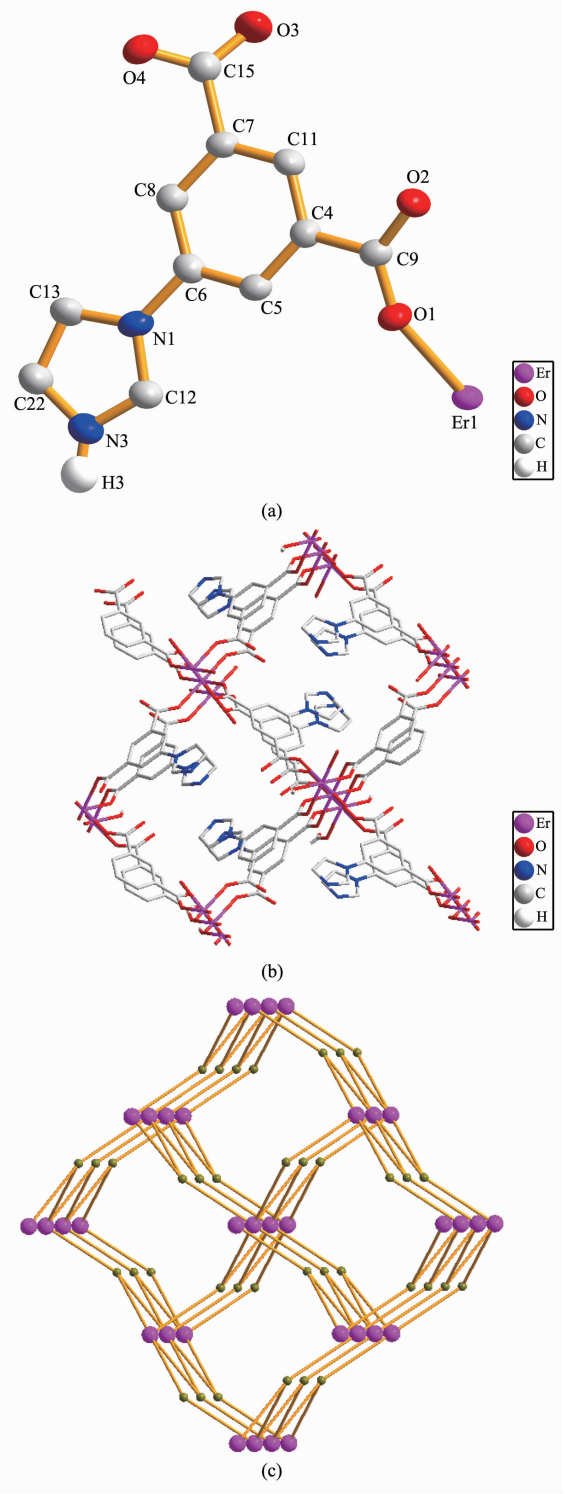

Fig.2 (a) Asymmetric unit of **2** with thermal ellipsoids at 50% probability level (the occupancy probability of H3 added to N3 is 0.5); (b) Packing structure of **2** along the *a* axis; (c) Topology of complex **2** (purple represents the 6-connected node of Er^{3+} ion and gray represents the 3-connected node of organic ligand)

nm. Complex **3** is a 2D network structure due to the planar ligand coordinating with Co^{2+} ion along three different directions, leading to -A-B-A-B- packing layers along the *c* axis (Fig.3b). Multiple π-π interactions can be found between the adjacent layers, with distances of 0.365 8 nm (between benzene rings) and 0.373 5 nm (between imidazole rings), respectively (Fig.S4), generating a 3D framework. Topologically, the framework can be interpreted as a 2D (3, 3)-connected net since every ligand coordinates with three Co^{2+} ions and each Co^{2+} ion connects three different ligands. Its Schläfli symbol is $(3^6.4^6.5^3)$ (Fig.3c).

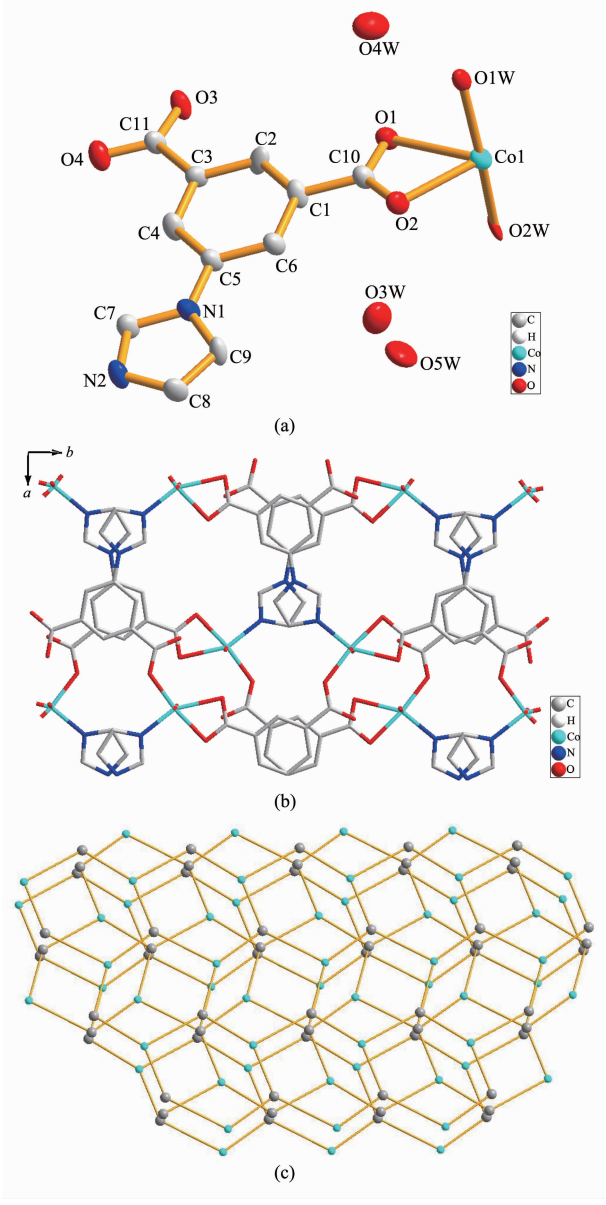

Fig.3 (a) Asymmetric unit of **3** with thermal ellipsoids at 50% probability level; (b) Packing structure of **3** along the *c* axis; (c) Topology of complex **3** (cyan represents the 3-connected node of Co^{2+} ion and gray represents the 3-connected node of organic ligand)

2.2 Comparison of the structures

Three coordination complexes of Pr(Ⅲ), Er(Ⅲ) and Co(Ⅱ) were successfully obtained by the reactions of the rigid ligand H_2L with the corresponding metal salts under the same conditions. The results show that the ligand adopts three different coordination modes in **1**, **2** and **3** (Fig.4). Usually, both O and N donors can coordinate with metal ions. However, since the Ln^{3+} ions prefer O- to N-donors, the ligand coordinates with Ln^{3+} ions in lanthanide complexes **1** and **2** through its two carboxyl groups, leaving the imidazole group free of coordination. Some N atoms of the imidazole group in these ligands are protonated. The carboxyl groups adopt monodentately and bidentately chelating modes in **1** (two ligands adopt different coordination modes), and monodentately and bidentately bridging modes in **2**, respectively. While in the transition metal complex **3**, besides the oxygen atoms of the carboxyl groups adopting monodentately and bidentately chelating mode, the nitrogen atom of the imidazole group also coordinates with Co^{2+} ions, resulting in a flat 2D network. Moreover, when lanthanide ions coordinate with ligands, usually, the bond direction is not determined, so the space resistance may become the major factor in determining the coordination modes[14]. The radius of Pr^{3+} ion is relatively 15% longer than that of Er^{3+}, which makes more space for oxygen atoms to coordinate with Pr^{3+} ion. This little difference generates two quite different structures, one is a 2D framework consisting of nine-coordinated Pr^{3+} ions, while the other is a 3D network with six-coordinated Er^{3+} ions. As mentioned above, when the imidazole group joins in coordination, the ligand L^{2-} turns into a rigid plane with three different coordinating directions, which tends to form a 2D framework.

2.3 Thermal analysis

Thermogravimetric analyses (TGA) were carried out for complexes **1**, **2** and **3** to determine their thermal stability. As shown in Fig.5, complex **1** exhibits

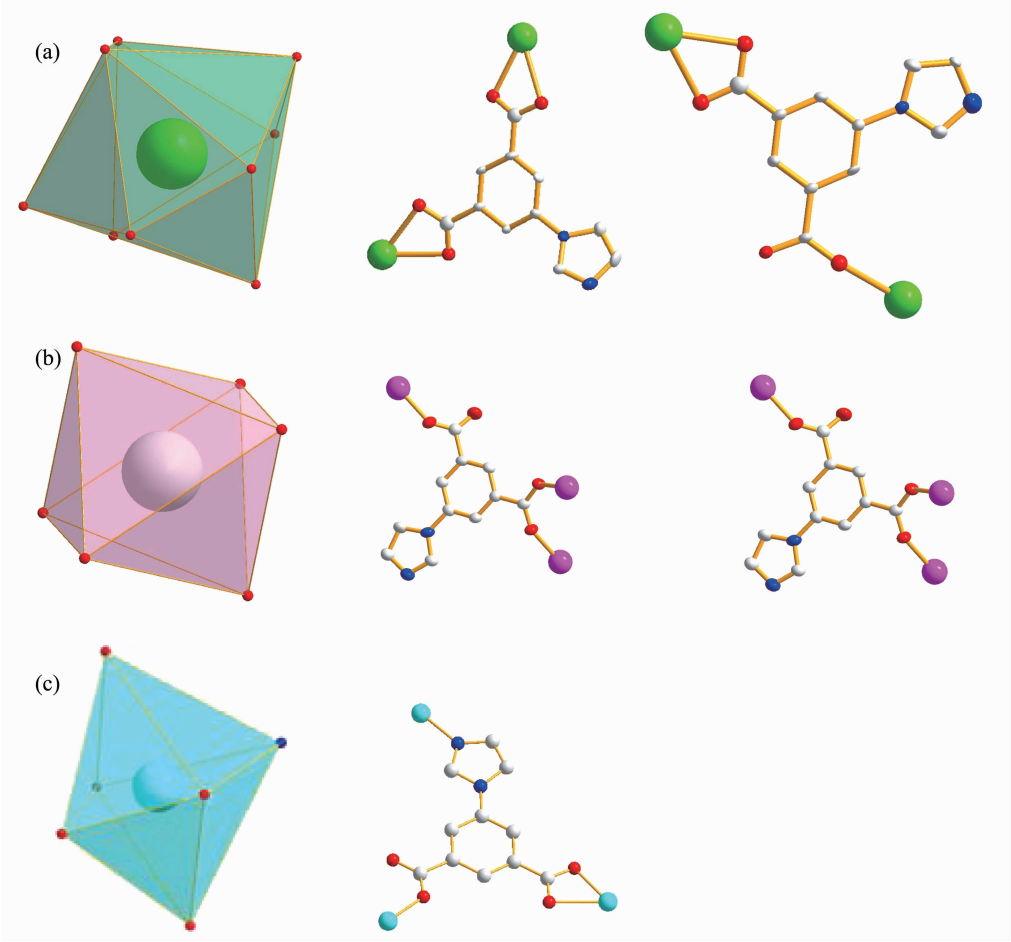

Fig.4　Coordination environment of the metal ions and the coordination modes of ligand in complexes **1** (a), **2** (b) and **3** (c)

a weight loss of 5.45% before 191 ℃, corresponding to the release of two water molecules (Calcd. 5.49%) in the structure. Then it slowly liberates its remaining coordinated water until 387 ℃ with a weight loss of 2.70% (Calcd. 2.74%). After that, it starts to decompose. For complex **2**, as mentioned above, the channel of the 3D structure is filled with the imidazole part, so there is no obvious weight loss before the whole structure collapses. Its framework can be stably sustained before 520 ℃. As for complex **3**, there are three successive and comparative weight loss process before 160 ℃. Its total weight loss of 15.03% is attributed to the liberation of one guest and two coordinated water molecules (Calcd. 15.23%). It will be collapsed when the temperature is higher than 390 ℃. From the decomposition temperature shown above, the three complexes exhibit good thermal stability. This is maybe due to their rigid framework and the multiple π-π interactions between the aromatic rings.

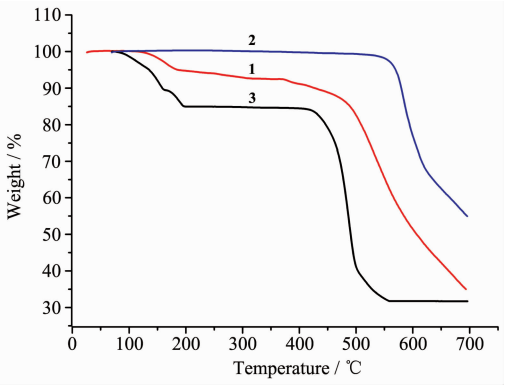

Fig.5　TG of complex **1**, **2** and **3**

3　Conclusions

Two lanthanide (Pr^{3+}, Er^{3+}) and one transition metal (Co^{2+}) coordination polymers based on the conjugated carboxylate-imidazole ligand L were successfully synthesized under similar hydrothermal conditions. The different nature of the metal ions makes the ligand adopts three different coordination modes,

resulting in three quite different structures. Compound **2** has a 3D structure, while compound **1** and **3** has a 2D layered structure, and this 2D structure is extended to 3D structure by the intermolecular π-π interactions between adjacent layers. All the complexes show good thermal stability.

Acknowledgments: Authors thank National Nature Science Foundation of China for financial support (No. 51173075). Authors also thank Professor Li Yi-Zhi and Doctor Zhai Lu for their kind help.

References:

[1] (a)Zheng B S, Bai J F, Duan J G, et al. *J. Am. Chem. Soc.*, **2011**,**133**:748-751
(b)Lu Z Z, Zhang R, Li Y Z, et al. *J. Am. Chem. Soc.*, **2011**, **133**:4172-4174
(c)Kim M, Cahill J F, Fei H H, et al. *J. Am. Chem. Soc.*, **2012**,**134**:18082-18088
(d)Kumar R, Kumar S, Kulandainathan M. *Microporous Mesoporous Mater.*, **2013**,**168**:57-64
(e)Mishra P, Edubilli S, Mandal B, et al. *Microporous Mesoporous Mater.*, **2013**,**169**:75-80

[2] (a)Zhang J P, Huang X C, Chen X M. *Chem. Soc. Rev.*, **2009**,**38**:2385-2396
(b)Hu Y X, Ma H B, Zheng B, et al. *Inorg. Chem.*, **2012**,**51**: 7066-7074
(c)Chen M, Bai Z S, Liu Q, et al. *CrystEngComm*, **2012**,**14**: 8642-8648

[3] (a)Kawano M, Kawamichi T, Haneda T, et al. *J. Am. Chem. Soc.*, **2007**,**129**:15418-15419
(b)Wang Y T, Fan H H, Wang H Z, et al. *Inorg. Chem.*, **2005**, **44**:4148-4150
(c)Carlucci L, Ciani G, Proserpio D, et al. *New J. Chem.*, **2003**,**27**:483-489
(d)Shin D M, Lee I S, Cho D, et al. *Inorg. Chem.*, **2003**,**42**: 7722-7724

[4] (a)Mahata P, Sundaresan A, Natarajan S. *Chem. Commun.*, **2007**:4471-4473
(b)Zhang J J, Wojtas L, Larsen R, et al. *J. Am. Chem. Soc.*, **2009**,**131**:17040-17041
(c)Wu S T, Long L S, Huang R B, et al. *Cryst. Growth Des.*, **2007**,**7**:1746-1752
(d)Zhu X, Sun P P, Ding J G, et al. *Cryst. Growth Des.*, **2012**,**12**:3992-3997
(e)Qin L, Hu J, Zhang M, et al. *Cryst. Growth Des.*, **2013**,**13**: 2111-2117

[5] (a)Chen S S, Chen M, Takamizawa S, et al. *Chem. Commun.*, **2011**,**47**:4902-4904
(b)Liu W, Yu J, Jiang J, et al. *CrystEngComm*, **2011**,**13**:2764 -2773
(c)Zhang J, Cheng S, Wang X, et al. *CrystEngComm*, **2013**, **15**:6074-6082

[6] (a)Li S L, Tan K, Lan Y Q, et al. *Cryst. Growth Des.*, **2010**, **10**:1699-1705
(b)Cui P, Ren L J, Chen Z, et al. *Inorg. Chem.*, **2012**,**51**: 2303-2310
(c)Jiang H L, Tatsu Y, Lu Z H, et al. *J. Am. Chem. Soc.*, **2010**,132:5586-5587
(d)Zhang Q A, Zhang J Y, Yu Q Y, et al. *Cryst. Growth Des.*, **2010**,**10**:4076-4084

[7] (a)Eddaoudi M, Li H, Yaghi O M. *J. Am. Chem. Soc.*, **2000**, **122**:1391-1397
(b)Eddaoudi M, Kim J, Rosi N, et al. *Science*, **2002**,**295**: 469-472
(c)Chae H, Siberio-Pérez D, Kim J, et al. *Nature*, **2004**,**427**: 523-527
(d)Millward A, Yaghi O M. *J. Am. Chem. Soc.*, **2005**,**127**: 17998-17999

[8] (a)Chen B, Ockwig N, Millward A, et al. *Angew. Chem. Int. Ed.*, **2005**,**44**:4745-4749
(b)Zhang J P, Chen X M. *J. Am. Chem. Soc.*, **2008**,**130**: 6010-6017
(c)Hu Y X, Xiang S C, Zhang W W, et al. *Chem. Commun.*, **2009**:7551-7553
(d)Tian D, Pang Y, Zhou Y H, et al. *CrystEngComm*, **2011**, **13**:957-966
(e)Wang L F, Kang L C, Zhang W W, et al. *Dalton Trans.*, **2011**,**40**:9490-9497

[9] (a)Chen S S, Lü G C, Fan J, et al. *Cryst. Growth Des.*, **2011**, **11**:1082-1090
(b)Chen S S, Zhao Y, Fan J, et al. *CrystEngComm*, **2012**,**14**: 3564-3576

[10]Cui K H, Yao S Y, Li H Q, et al. *CrystEngComm*, **2011**,**13**: 3432-3437

[11]*Software Packages SMART and SAINT*, Siemens Analytical X-ray Instrument Inc., Madison: WI, **1996**.

[12]Sheldrick G M. *SHELX*-97, *Program for the Refinement of Crystal Structure*, University of Göttingen, Göttingen, Germany, **1997**.

[13]Carter K, Pope S, Cahill C. *CrystEngComm*, **2014**,**16**:1873-1884

[14]Zhou X Y, Guo Y L, Shi Z H, et al. *Dalton Trans.*, **2012**,**41**: 1765-1775